MODULATION OF NEGATIVE WORK OUTPUT FROM A STEERING MUSCLE OF THE BLOWFLY *CALLIPHORA VICINA*

MICHAEL S. TU AND MICHAEL H. DICKINSON

Department of Organismal Biology and Anatomy, The University of Chicago, 1025 East 57th Street, Chicago, IL 60637, USA

Summary

Of the 17 muscles responsible for flight control in flies, only the first basalar muscle (b1) is known to fire an action potential each and every wing beat at a precise phase of the wing-beat period. The phase of action potentials in the b1 is shifted during turns, implicating the b1 in the control of aerodynamic yaw torque. We used the work loop technique to quantify the effects of phase modulation on the mechanical output of the b1 of the blowfly *Calliphora vicina*. During cyclic length oscillations at 10 and 50 Hz, the magnitude of positive work output by the b1 was similar to that measured previously from other insect muscles. However, when tested at wing-beat frequency (150 Hz), the net work performed in each cycle was negative. The twitch kinetics of the b1 suggest that negative work output reflects intrinsic specializations of the b1 muscle. Our results suggest that, in addition to a possible role as a passive elastic element, the phase-sensitivity of its mechanical properties may endow the b1 with the capacity to modulate wing-beat kinematics during turning maneuvers.

Introduction

The flight musculature of flies consists of two specialized muscle groups which differ both anatomically and in their mode of neural control (Pringle, 1949). The fibrillar, indirect flight muscles constitute the largest volume of musculature in the thorax and function almost exclusively to generate power for flight. These large, asynchronous muscles are stretch-activated such that the timing of contractions is determined by mechanical oscillations of the thorax and not by the arrival of neural excitation. Although flies may modulate the spike frequency in the indirect muscles, these muscles do not function in the fine control of turning (Heide, 1983). Instead, flight maneuvers are controlled by 17 pairs of synchronous steering muscles (Heide, 1968, 1971; Wisser and Nachtigall, 1984), in which contractions follow motor axon action potentials in the conventional one-to-one manner. Although the steering muscles constitute a tiny fraction of the total volume of flight musculature, they are crucial in enabling flies to execute rapid and complex flight maneuvers.

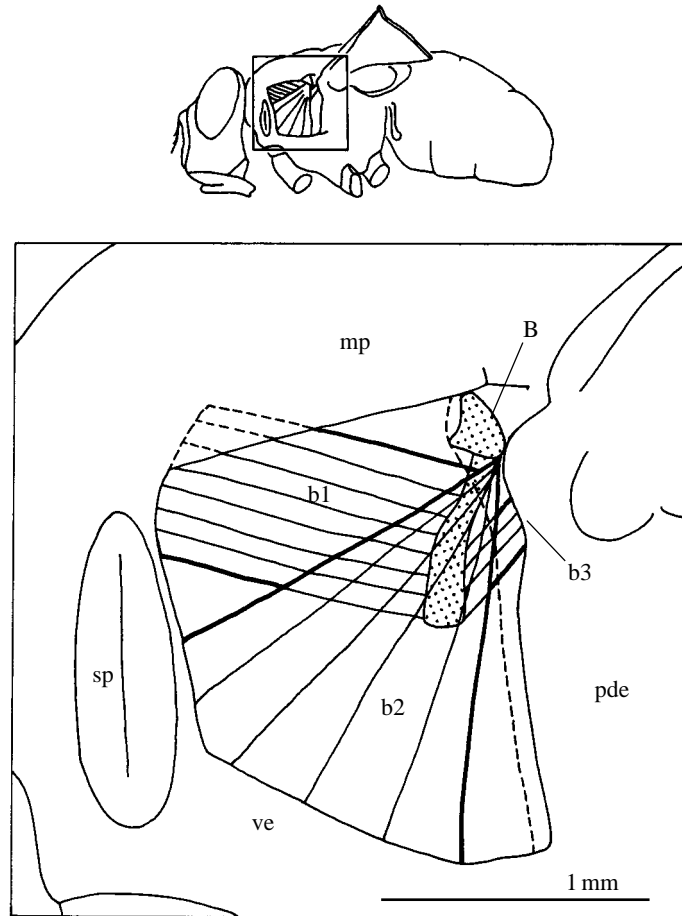The unique properties of the first basalar muscle (b1; Fig. 1; muscle nomenclature

Fig. 1. Lateral view of *Calliphora vicina* with the anterior dorsal episternum removed to expose the basalar muscles. The basalare (B) sends a rod-like projection into the thorax forming the insertions of the first (b1) and third (b3) basalar muscles. The b1 is rectangular in lateral view and inserts anteriorly on the thoracic cuticle. The most lateral of the basalar muscles, the second basalar (b2), inserts on the basalare at a point near its outer, triangular region. The b1 and b2 extend the wing by pulling the basalare forwards and upwards around its points of articulation on the mesopraescutum (mp) and the posterior margin (dashed line) of the anterior dorsal episternum. A flexible membrane separates the anterior dorsal episternum and the posterior dorsal epistermum (pde). ve, ventral episternum; sp, spiracle. Nomenclature of thoracic sclerites follows Wisser and Nachtigall (1984).

follows Heide, 1968) suggest that it plays an important role in both course stabilization and voluntary turning maneuvers. Of the steering muscles for which activity patterns have been recorded during tethered flight, only the b1 and the pleuro-sternal muscle (ps1) fire continuously. The remaining steering muscles are selectively activated only during turning maneuvers (*Calliphora* and *Musca:* Heide, 1971, 1975, 1983). Whereas the ps1 fires tonically at a rate well below wing-beat frequency (*Calliphora:* Kutsch and Hug,

1981), the b1 is the only muscle known to fire a phase-locked action potential each and every wing beat in every fly species so far examined (*Drosophila*, Ewing, 1979*a*,*b*; Götz, 1983; Heide, 1983; *Calliphora*, Heide, 1971, 1975, 1983; Kutsch and Hug, 1981; *Musca*: Heide, 1975; Egelhaaf, 1989). In addition, only the b1 is known to undergo shifts in its firing activity such that action potentials are advanced in phase during turns to the contralateral side (Heide, 1983; Götz, 1983; Egelhaaf, 1989). This phase shift makes the b1 a likely candidate for the control of one component of steering behavior, termed the ventral flip, the rapid supination of the wings at ventral stroke reversal (Dickinson *et al.* 1993). As with the timing of b1 action potentials, the timing of the ventral flip is advanced in phase during turns to the contralateral side. Control of the b1 firing pattern by wing-beat synchronous afferents (Heide, 1983; Miyan and Ewing, 1984) and the exceptionally large size of the b1 motor axon in *Drosophila* (King and Tanouye, 1983) and *Calliphora* (Heide, 1983) strongly suggest that rapid activation and low temporal variance are critical design characteristics of this sensorimotor system. These properties are consistent with a role for the b1 in controlling the rapid, wing beat by wing beat, adjustments in ventral flip timing (Dickinson *et al.* 1993).

Despite its potential importance for flight control, neither the mechanical output of the b1 nor its capacity for modulation has been characterized under conditions relevant to flight. The b1 is innervated by two axons: the enormous, presumably glutaminergic, excitatory cell and a small accessory fiber of unknown function. Aside from possible long-term modulation *via* the accessory cell, control of the b1 output does not occur through selective recruitment of multiple motor units. Under isometric conditions, stimulation at wing-beat frequency has been reported to result in nearly complete tetanus of the b1 (Heide, 1971; Bergmann-Erb and Heide, 1990). The b1, however, does not function isometrically during flight, but undergoes cyclic length oscillations at wing-beat frequency because of its mechanical connections to the wing hinge (Nalbach, 1989). Because the b1 is continuously active and is limited to a single action potential each wing beat, shifts in activation phase may be the only means by which the nervous system can rapidly modulate the muscle output.

In this study, we employed the work loop technique in order to quantify the output of the b1 under conditions simulating flight using the blowfly *Calliphora vicina*. This approach, first used by Machin and Pringle (1960) and later modified for synchronous muscles by Josephson (1985), allows one to measure the mechanical output of a muscle undergoing phasic stimulation and cyclic changes in length. Previous work loop studies have focused on muscles involved in locomotion, ventilation or sound production, activities in which muscles must generate significant mechanical power (Josephson, 1993). The steering muscles of flies, however, function primarily in locomotor control. Consequently, the capacity for rapid modulation of the mechanical properties, rather than the magnitude of power production, may be their most important functional characteristic.

Materials and methods

Animals

We used adult *Calliphora vicina* (mean mass 0.082 g, *N*=43) from a laboratory culture

maintained under conditions of ambient light and temperature (19–25 °C). Flies were used for experiments 7–14 days after emergence.

Motor axon morphology

We anesthetized flies by chilling them for 4–6 min at −4 °C. The flies were hemissected in the sagittal plane and secured with Takiwax (Central Scientific), cut surface uppermost, to the bottom of a Petri dish. The indirect muscles were picked away to expose the b1 without disturbing its insertions. We then cut the wing nerve containing the b1 motor axon where it leaves the thoracic ganglion and pulled the cut end into a Vaseline well filled with fluorescein-conjugated dextran (100 mg ml^{-1} 0.2 % KCl; Molecular Probes, Inc.). The muscle was moistened as necessary with insect saline (140 mmol l^{-1} NaCl, 5 mmol l^{-1} KCl, 7 mmol l^{-1} CaCl$_2$, 1 mmol l^{-1} MgCl$_2$, 4 mmol l^{-1} NaHCO$_3$, 4.3 mmol l^{-1} Tris–HCl, 0.66 mmol l^{-1} Tris base, 5 mmol l^{-1} trehalose; pH 7.3). We allowed the nerve to fill for 2 h at room temperature. The nerve and muscle were fixed for 2 h in 4 % paraformaldehyde in phosphate-buffered saline (PBS) (0.1 mol l^{-1}, pH 7.2) followed by a wash in buffer. We then dissected the b1 and its motor axon free from the surrounding tissue. Finally, the nerve and muscle were dehydrated in ethanol, cleared in xylene, and mounted for microscopic examination.

Force measurements

The force transducer consisted of a cantilevered beam cut from 0.50 mm phosphor-bronze shim stock (Fig. 2). We soldered a small clamp to one side of the free end and attached a small mirror to the opposite side. Light from a helium–neon laser was reflected by the mirror and projected onto the surface of a position-sensing photodiode (UDT Sensors Inc., SL series). Beam deflection caused the reflected laser light to traverse the sensing surface of the photodiode, producing a voltage signal linearly related to the applied load. The force beam compliance was 3.3×10^{-5} m N^{-1}, and its resonant frequency was 600 Hz.

Specimen preparation

After removing the legs and wings from the anesthetized fly, we glued the fly, left side up, to a Plexiglas stage (Fig. 2) using dental cement (Opotow). The Plexiglas stage was mounted on a magnetic coil oscillator (Ling Dynamic Systems). The b1 muscle is flat, approximately rectangular and extends from the anterio-dorsal wall of the thoracic capsule to the anterior surface of the basalare (Fig. 1). Anterio-dorsal rotation of the basalare in the quiescent fly results in extension of the wings (Nalbach, 1989). We solidly embedded the region near the anterior origin of the b1 muscle in dental cement to minimize local deformation of the cuticle. We left the anterior dorsal episternum intact in order to avoid disruption of the underlying tracheal supply to the muscle (nomenclature of thoracic sclerites follows Wisser and Nachtigall, 1984). We exposed the insertions of the three basalar muscles on the basalare by cutting away the wing hinge and the membrane separating the anterior and posterior episterna. To isolate the b1, we cut the second basalar muscle (b2) at its insertion on the basalare and severed the tendinous attachment of the third basalar muscle (b3) to the anterior tergal lever. Finally, we pulled the basalare
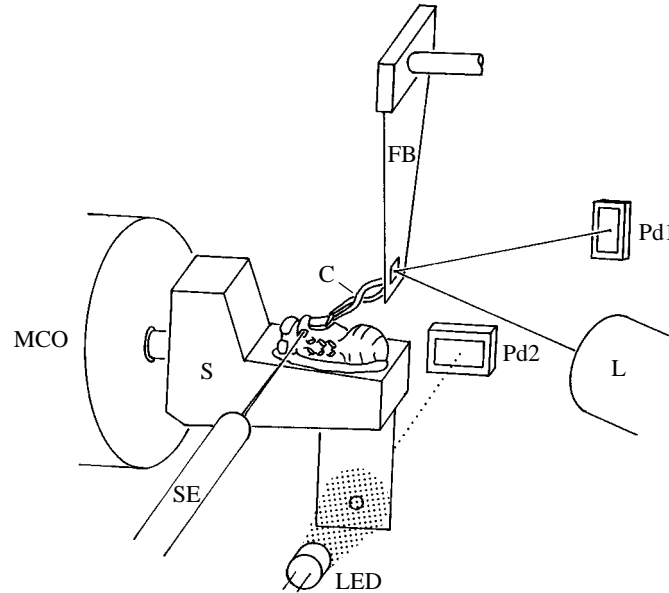
Fig. 2. Schematic diagram of the apparatus used to measure muscle forces during cycles of length oscillation and phasic stimulation. The fly was glued to the stage (S) mounted on a magnetic coil oscillator (MCO). The end of the b1 inserting on the basalare was dissected free and secured to the force beam (FB) *via* a clamp (C). Deflection of the force beam, measured with a laser (L) and position-sensing photodiode (Pd1), was calibrated to yield measurements of muscle force. The magnetic coil oscillator sinusoidally translated the fly and anterior b1 muscle insertion relative to the fixed end of the muscle clamped to the force beam. Length oscillations of the b1 were measured using an infrared-emitting diode (LED) and position-sensing photodiode (Pd2) positioned under the stage. The stimulating electrode (SE) was inserted through a small hole and hooked around the nerve containing the motor axon to the b1. For clarity, the b1 is shown exposed. During actual experiments, however, the episternum overlying the b1 was left intact.

free of its attachments to the surrounding cuticle, and secured it in the clamp of the force transducer.

Muscle stimulation and intracellular recordings

We fashioned the stimulating electrode from tungsten wire, electrolytically etched and bent into a fine hook. The electrode was inserted through a hole cut in the ventral episternum and hooked around the nerve containing the motor axons of the basalar muscles (Fig. 2). We inserted a ground electrode into the thorax near the anterior insertion of the b1 muscle. The stimulus duration ($20\,\mu$s) and intensity (1.1–2.8 times threshold) were adjusted to the minimum values required to obtain consistent activation of the muscle at 150 Hz. Often, stimuli delivered to the nerve also activated the pleuro-sternal muscles. However, in preparations in which the b1 muscle failed, continued contraction of the pleuro-sternal muscles did not produce forces detectable by the force transducer. In some preparations, we recorded intracellular action potentials using $40\,$MΩ

glass micropipettes filled with $3\,mol\,l^{-1}$ KCl. Signals were amplified (A-M Systems, model 1600) and recorded on a digital oscilloscope (Nicolet 410).

Muscle length and strain

Throughout each experiment, the posterior insertion of the b1 was clamped to the force beam and remained stationary (Fig. 2). The anterior insertion of the b1 remained attached to the fly, which was in turn secured to the Plexiglas stage. The oscillator drove the stage back and forth, thereby oscillating the muscle length by moving the anterior insertion in the fly relative to the posterior insertion clamped to the force beam. To allow precise adjustment of muscle length, we mounted the oscillator assembly on a fine translation stage. After clamping the b1 to the force beam, we used exoskeletal landmarks to adjust the muscle length to the resting length. We define resting length as the length that approximates as closely as possible the length of the b1 in the quiescent fly. Sinusoidal length changes were applied symmetrically about the resting length. Strain refers to the total percentage change in muscle length during an oscillation cycle: strain = 100(maximum length − minimum length)/resting length. For measuring changes in muscle length, we attached an aluminum sheet with a circular hole to the Plexiglas stage holding the fly. A position-sensing photodiode (UDT Sensors Inc., SL series) produced a voltage output proportional to the position of the infrared light beam projected through the hole in the aluminum sheet.

Experimental protocol

In each preparation, we examined the effects of stimulus phase in combination with either cycle frequency or strain magnitude. The function generator driving the oscillator triggered a single stimulus to the muscle during each cycle. We adjusted stimulus phase by introducing a variable delay between the trigger pulse and the stimulus. The delay was adjustable in increments of $10\,\mu s$. An experimental series consisted of 20 bursts of stimulation and sinusoidal length change, each lasting 35 cycles. During the 15 s interval separating each burst, we adjusted the stimulus phase to a new value. Frequency, amplitude and average muscle length remained constant throughout each experimental series while we varied stimulus phase from 0° to 360° in twenty 18° increments. We moistened the muscle and nerve as necessary with insect saline. Within each experimental series, values of frequency, strain, muscle length and the sequence of phase values were chosen in random order. Each series was immediately preceded and followed by two bursts of length oscillation without stimulation, two bursts of stimulation without length oscillation and two recordings of muscle force during single isometric twitches. We performed one set of experiments to examine the effects of stimulus phase and strain at 150 Hz, the approximate wing-beat frequency of *Calliphora* during flight (Ennos, 1989; Kutsch and Hug, 1981). Another set of experiments was performed at 10, 50, 100 and 150 Hz to examine the effects of oscillation frequency on work output. All experiments were performed at 20–23 °C.

Preparations remained viable without a noticeable decline in performance for up to 1 h. Any significant damage to the tracheae invariably resulted in either poor initial performance or rapid failure of the preparation. We terminated data collection if the

condition of the preparation deteriorated noticeably. Decline in a successful preparation was indicated by a large and rapid reduction in force output and a failure to follow stimulation in a one-to-one manner. For each preparation we collected data from a maximum of eight experimental series of 20 phase values, requiring approximately 50 min to complete.

Muscle dimensions

Before removing the fly from the apparatus at the conclusion of each experiment, we removed the left anterior dorsal episternum. With the muscle clamped to the force transducer, an ocular micrometer was used to measure the length of the left b1 muscle to the nearest 0.03 mm. We then measured thorax length, here defined as the length along the dorsal midline of the thorax, from the posterior margin of the mesoscutum to the transversal ridge.

The b1 of *Calliphora* is too small to weigh reliably. Because the b1 is a flat rectangular muscle with nearly constant width and thickness along its length, reliable measurements of length and cross-sectional area could be used to calculate muscle volume accurately. We could accurately measure muscle length *in situ* as described above. Unfortunately, because the muscle is so small, attempts to section muscles used in experiments were often unsuccessful or produced highly variable measurements of cross-sectional area. Consequently, we performed a morphometric analysis on a group of flies specifically for the purpose of obtaining a relationship between an easily measured variable (thorax length) and muscle volume.

Cold-anesthetized flies were decapitated, and the legs, wings and abdomens removed. We used an ocular micrometer to measure thorax length, as defined above. We carefully picked away cuticle in order to expose the basalar muscles without disrupting the articulation of the basalare. On each side of the thorax, we cut the b2 at its dorsal insertion and measured the length of the b1. We embedded each thorax in OCT compound on the quick-freeze stage of a cryostat. Each thorax was sectioned to obtain 20μm transverse sections of the b1 muscles. We cut out and weighed *camera lucida* tracings of muscle sections to obtain measurements of muscle cross-sectional area. Using linear regression, we obtained a relationship between thorax length, (L_t, mm) and muscle volume, (V_m, mm^3): $V_m=0.06L_t-0.08$, $r^2=0.33$, $N=38$. The slope of this relationship was significantly different from zero (*t*-test, $P=0.0002$). We used the regression to calculate the volume of muscles used in the work loop experiments. From the predicted volume we calculated an estimate of muscle mass, assuming a muscle density of $1 \mathrm{g\,cm}^{-3}$. We also estimated cross-sectional area by dividing volume by the measured muscle length. The b1 muscles from successful work loop experiments had a mean length of 1.04±0.25 mm (S.D.) and a mean estimated mass of 42.6 ±7.5 μg (S.D.), $N=17$.

Data acquisition and analysis

Data were collected by a 12-bit analog to digital converter (PCL-718, Advantech) controlled by a computer (486SX/25). At each frequency, we adjusted the sampling rate to maintain a constant 60 data points per cycle for each channel. Force and length data for isometric twitches were each digitized at a rate of 10 kHz. Raw data were digitally filtered

with zero phase delay and a cut-off frequency of 1 kHz. From single isometric twitches, we measured the peak force and the following time intervals: stimulus to onset of force, onset of force to peak force, peak force to 50 % relaxation, and peak force to 90 % relaxation. For each experimental series, we calculated the projected delay (D_{onset}) between stimulation of the motor axon and the onset of force by averaging values from four single twitches, two preceding and two following the experimental series. We then calculated the phase of activation (hereafter, phase) for each burst within the experimental series: phase = (D_{stim} + D_{onset})/cycle period $\times$ 360˚, where D_{stim} is the delay between the start of lengthening and muscle stimulation. Therefore, phase values represent the projected delay between the start of lengthening and the onset of contraction, expressed in degrees. We calculated the net work per cycle from force and length data averaged over the last 20 cycles of each burst. In all data presented here, final values of force and displacement in the cycle-averaged data were within 5 % of their respective initial values. We integrated muscle force with respect to muscle length over one cycle period to obtain the net work performed per cycle. This value equals the area enclosed by the loop formed by plotting force against muscle length for one cycle period, as described by Josephson (1985).

Results

Motor axon morphology

Fluorescein dye applied to the cut end of the wing nerve filled a single large motor axon terminating on the b1 muscle (Fig. 3). This axon has a diameter of approximately 25 μm. We rarely observed an accessory axon, presumably because of the short filling times. The arborization of the motor axon is extensive, with branches distributed evenly over the entire surface of the muscle. The greatest distance between varicosities is approximately 30 μm.

Isometric properties

Each stimulus above threshold elicited a single, overshooting action potential in the b1 muscle (Fig. 4A). The mean delay between stimuli delivered to the motor axon and the onset of force generation was 2.1±0.3 ms (s.d., N=256). Rise time, measured from onset to peak force, was 7.0±1.5 ms. The time from onset to 50 % relaxation was 18.9±7.1 ms, and from onset to 90 % relaxation, 51.3±28.0 ms. The mean peak isometric force was 13.9±3.8 mN, corresponding to 40±10 N cm^{-2}. Stimulation at 150 Hz did not result in complete tetanus (Fig. 4B). The mean tension in the b1 during stimulation at 150 Hz was 29±10 mN (s.d., N=118), corresponding to a stress of 83±29 N cm^{-2}.

Phase of muscle activation

In the absence of a direct measure of muscle activation with respect to time, we chose to define phase in terms of the projected time to force onset. The correction applied to the raw stimulus phase should account for conduction time and synaptic delays without involving assumptions regarding the time course of force generation under dynamic conditions. By our definition, phase operationally identifies a set of experimental
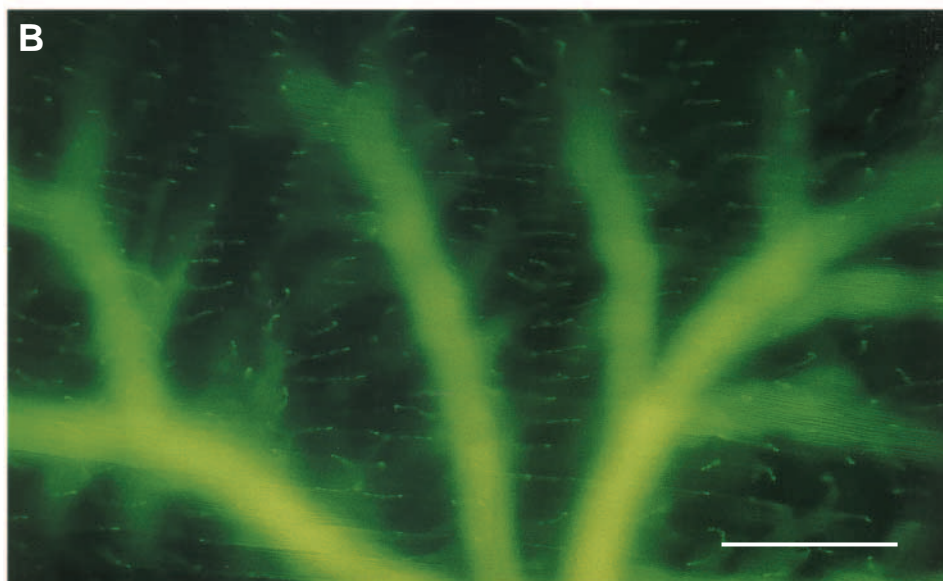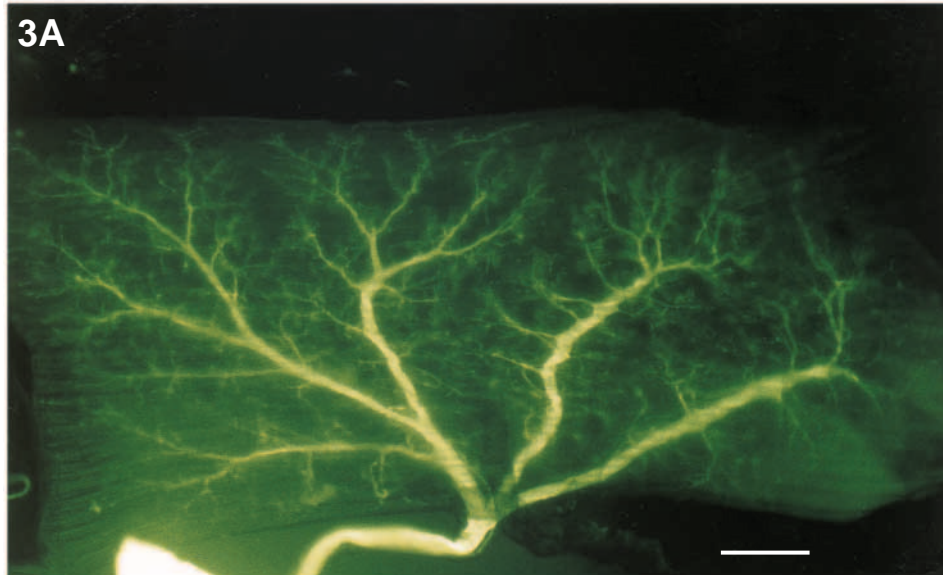
Fig. 3. Extensive arborization of the b1 motor axon suggests specializations for rapid activation of the muscle. (A) Whole mount of the b1. The motor axon has been filled with a fluorescein-conjugated dextran. The axon diameter is approximately $25\,\mu$m. Axon terminals are evenly dispersed over the entire muscle. (B) Higher magnification view of another preparation, focused on the outer layer of muscle fibers. The greatest distance between varicosities is approximately $30\,\mu$m. Scale bars, $100\,\mu$m.
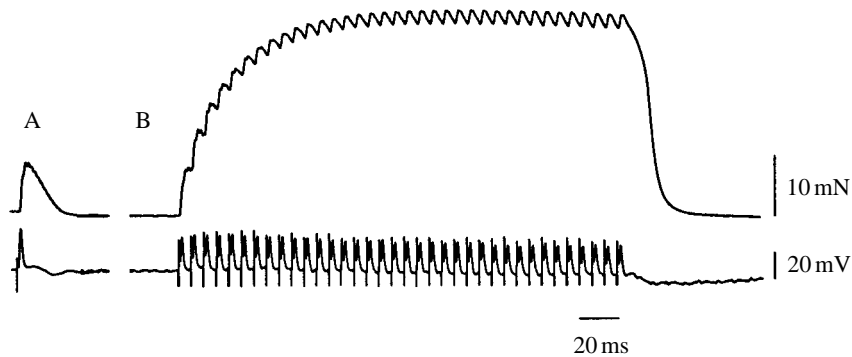
Fig. 4. Isometric twitches of the b1 do not fuse completely during stimulation at wing-beat frequency. Muscle force (upper traces) and action potentials (lower traces) were measured under isometric conditions. (A) Single twitch and action potential. (B) Force and action potentials recorded during stimulation at 150 Hz.

variables associated with a specific response of the muscle. At any one frequency, similar phase values should be directly comparable. However, corresponding points of the work *versus* phase relationships, such as the maximum and minimum values of work, were consistently shifted to earlier phases for each increase in frequency (see below, Fig. 6). This phase shift may have arisen in part as a result of the manner in which we defined activation phase. Neglecting the summed effects of successive stimuli, and assuming that the time course of muscle activation remains largely independent of cycle frequency, then the calculated phase should underestimate the timing of similar states of activation relative to the cycle period at higher frequencies. However, a definition of phase based on the projected time of peak isometric twitch force did not produce a more consistent alignment of the work *versus* phase relationships at different frequencies.

Work output at 10, 50, 100 and 150 Hz

We measured work output at different frequencies from eight successful preparations at strains of 1 % and 2 % resting length. Sinusoidal strains at 10 Hz without stimuli resulted in nearly sinusoidal fluctuations in muscle force (Fig. 5, F_{S-}). Stimuli delivered once per cycle at 10 Hz produced discrete force transients superimposed on patterns of muscle force similar to those recorded from the unactivated muscle (Fig. 5, F_{S+}). Stimulation near the onset of shortening resulted in counter-clockwise work loops, corresponding to net positive work output (Fig. 5, S+). At 100 and 150 Hz, stimuli did not elicit discrete force transients, and variations in muscle force, with or without stimulation, were approximately sinusoidal in response to imposed strains. At these frequencies, the predominant effect of stimulation was a tonic increase in the dynamic stiffness, indicated by an increase in the ratio of peak force to peak strain (Fig. 5, compare S− and S+). The mechanical response of the muscle at 100 Hz or higher resembled that of a passive element: clockwise work loops reflect net mechanical energy absorption during each cycle. At 50 Hz, muscle forces consisted of small force transients superimposed on oscillations approaching the nearly sinusoidal response observed at 100 and 150 Hz.
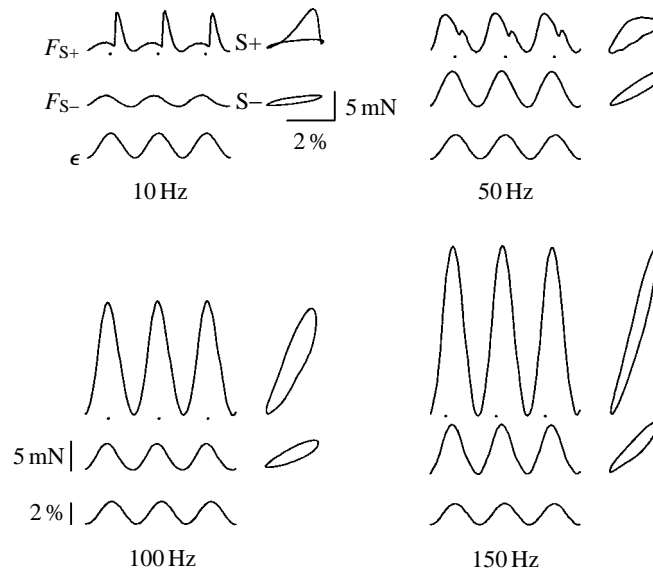
Fig. 5. Muscle force and strain during sinusoidal length oscillations at 10, 50, 100 and 150 Hz. The three left-hand traces in each panel show muscle strain (ϵ), muscle force during length oscillations without stimulation (F_{S-}) and muscle force during length oscillations with stimulation (F_{S+}) plotted as functions of time. The time scale at each frequency has been normalized to the cycle period. The force and strain scales are the same for each frequency. The times of stimuli delivered to the motor axon are indicated by dots below traces of muscle force. The traces on the right in each panel show work loops formed by plotting the cycle average of muscle force against strain, with stimulation (S+) and without stimulation (S−). Force (ordinate) and strain (abscissa) scales are the same for all work loops. The data are from a single preparation. At each frequency shown, the phase of the projected onset of muscle force was 204 °, the optimum phase for positive work output at 10 Hz and 2 % strain. The work loop shown at 10 Hz was counter-clockwise, indicating that the muscle performed net positive work per cycle. At the phase shown, the net work per cycle was negative at 50, 100 and 150 Hz.

At all frequencies tested, work output varied through a single minimum and single maximum value as the phase of activation was varied from 0 ° to 360 ° (Fig. 6). The b1 muscle performed the greatest net positive work over the largest phase range at 10 Hz. The magnitude and range of positive work output declined at 50 Hz. At 100 and 150 Hz, the net work output was negative for all values of activation phase, even at strains as small as 1 % resting length. At all frequencies there was variation in the maximum work output between preparations and, in a few cases, the work output was negative at 10 and 50 Hz. We do not know whether these negative values represent normal variation in muscle performance or the effects of damage to the muscle or tracheal system during preparation. Values of peak work output from all preparations at 10, 50, 100 and 150 Hz are summarized in Fig. 7.

Effects of strain magnitude on work output at 150 Hz

At 150 Hz, we measured work output at six strain magnitudes ranging from 0.3 to
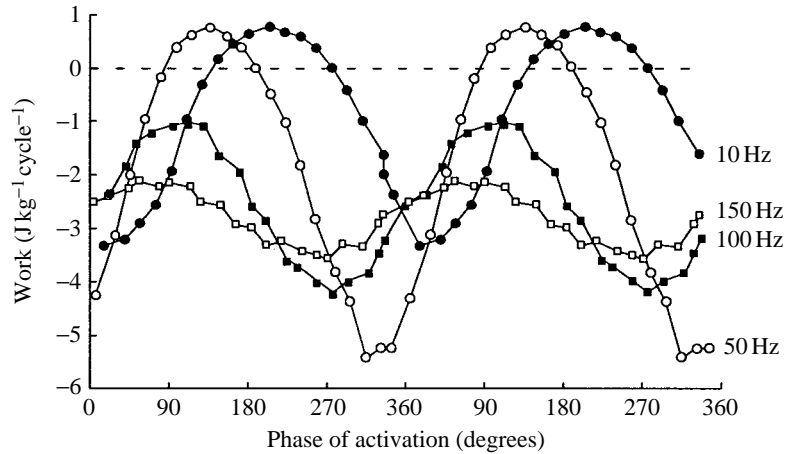
Fig. 6. The b1 can generate positive work at 10 and 50 Hz. Work output from a single preparation at 10, 50, 100 and 150 Hz is plotted as a function of activation phase. The strain amplitude was 2 % of resting length. To clarify the cyclic nature of the data, we have plotted the same data set over two phase cycles.
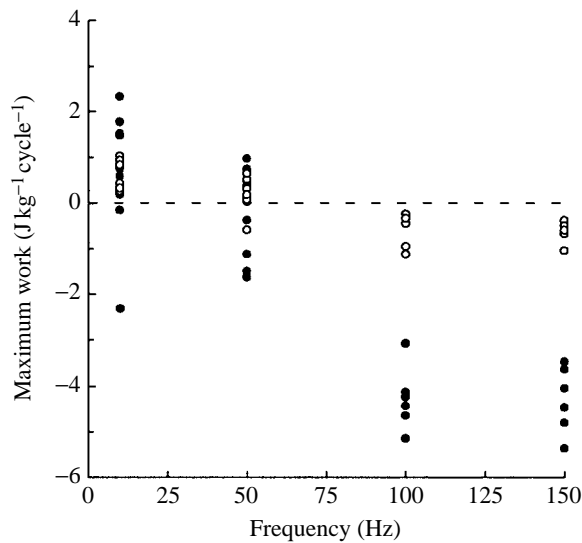

Fig. 7. Work output by the b1 muscle became negative at frequencies between 50 and 100 Hz. The graph shows the maximum work output for each experimental series of 20 phase values at 10, 50, 100 and 150 Hz. Data have been pooled from eight preparations. Strain magnitudes are 1 % (open circles) and 2 % (filled circles).

11.1 % in each of nine successful preparations. Work loops were clockwise at all values of strain and activation phase, showing that the net work output per cycle was negative (Fig. 8). Variation in the peak-to-peak amplitude of force in each cycle primarily reflected changes in the maximum force. The minimum force for each cycle remained
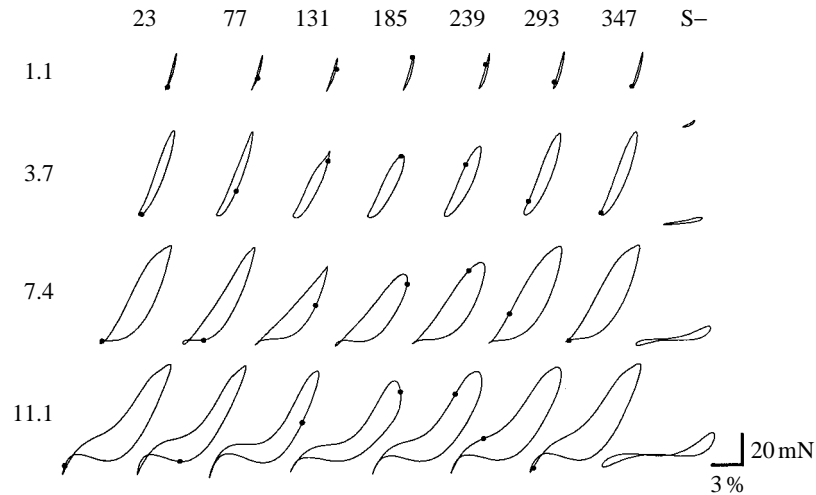
Fig. 8. Work loops at 150 Hz. All work loops run clockwise, indicating net energy absorption in each cycle. Each row contains work loops from one experimental series at the strain indicated on the left. The position of the work loops on the force axis (ordinate) is the same for all work loops in any one row. Numbers at the top of the figure indicate the phase of activation for work loops in each column. The projected time of active force generation is also indicated by a dot on each work loop. Work loops for the unstimulated muscle (S−) are shown on the right. The data are from a single preparation. Stimulation during length oscillations at wing-beat frequency greatly increased both the net energy absorption per cycle and the dynamic stiffness of the b1. The net energy absorption (enclosed area), patterns of change in muscle stiffness (slope of the force–length relationship) and the peak force in each cycle varied with changes in stimulus phase at each strain magnitude.

relatively constant at all values of activation phase (Fig. 8). The shape and size of the work loops differed at different phase values, indicating that changes in phase altered the dynamics of muscle force within each strain cycle. At all but the smallest strains, the response of the muscle was non-linear; force fluctuations were not sinusoidal in response to sinusoidal strains. Consequently, we could not easily describe the response of the b1 in terms of a simple linear model with a single dynamic modulus composed of viscous and elastic terms (e.g. Meyhöffer and Daniel, 1990). Variation in the dynamic stiffness throughout each cycle can be seen qualitatively as a departure of each work loop from a perfect ellipse (Fig. 8). Changes in the shape of the work loops indicate that the dynamic changes in stiffness during each cycle depended on the phase of activation.

At each strain, energy absorption went through a single maximum and a single minimum value as stimulus phase varied from 0 to 360° (Fig. 9). Strain magnitude affected both the mean work output and the amplitude of work modulation in response to phase variation (Fig. 10). With increasing strain, the mean energy absorption increased to a greater extent for muscles receiving phasic stimulation than for unstimulated muscles (Fig. 10A). In addition, changes in the phase of activation produced a larger difference between the maximum and minimum of energy absorption as strain magnitude was increased (Fig. 10B).
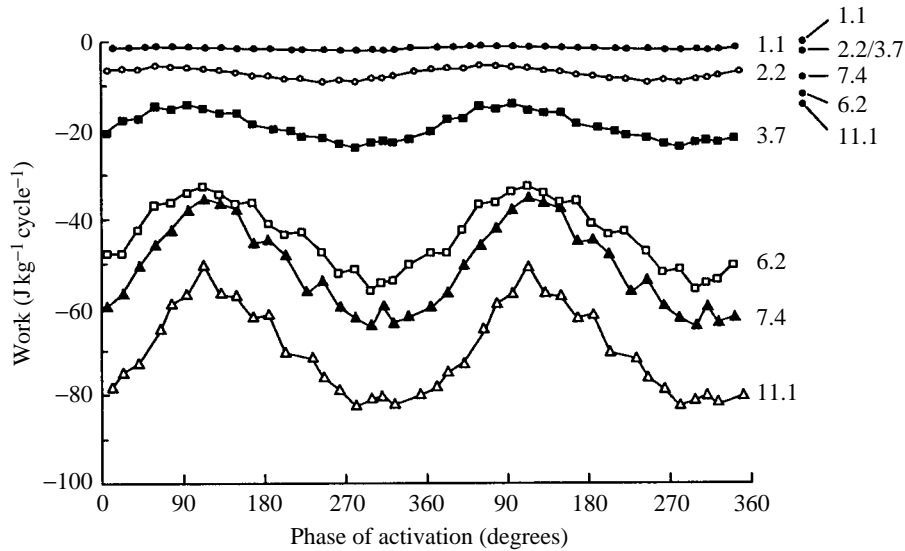
Fig. 9. Work output at 150 Hz was negative at all strain magnitudes and all values of activation phase tested. The magnitude of energy absorption, however, was sensitive to changes in the phase of activation. The graph shows negative work output from a single preparation at 150 Hz as a function of activation phase. Each curve represents data from one experimental series. The number immediately to the right of each data set indicates the strain magnitude for that series. The filled circles at the upper right represent the magnitude of work absorbed by the unstimulated muscle at the indicated strain. As in Fig. 6, the data set is plotted over two cycles.
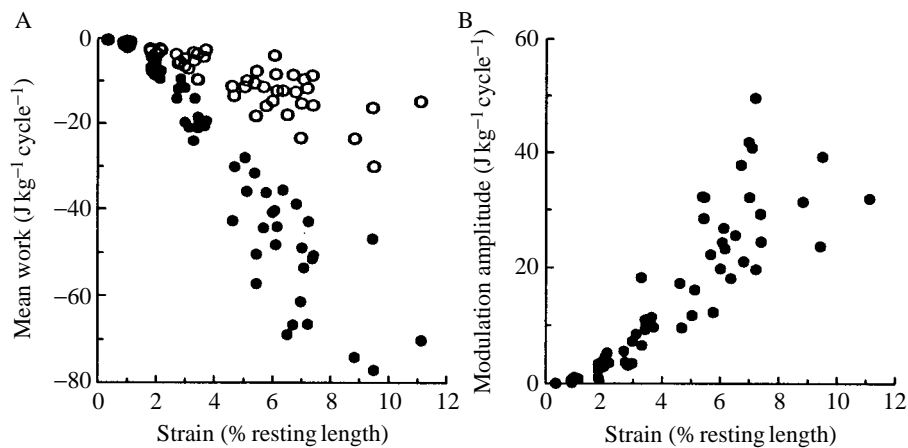

Fig. 10. The work output decreased and the phase-dependent work modulation increased with increasing strain magnitude. (A) The mean work is the average work output of the b1 at the 20 phase values of each experimental series. Filled circles represent mean values of work output from muscles receiving phasic stimulation. The level of energy absorption by unstimulated muscles is shown for comparison (open circles). (B) The amplitude of work modulation is the range between the maximum and minimum work output at the 20 phase values in each experimental series. (For example, it is the range between the maximum and minimum values of work output at each strain in Fig. 9.)

Discussion

The highest frequency at which the b1 performed net positive work per cycle was between 50 and 100 Hz, substantially below wing-beat frequency. At frequencies relevant for flight, the net work performed by the b1 muscle was negative at all amplitudes and all phase values tested. Although the work output was negative when measured at wing-beat frequency, the magnitude of energy absorption, the peak force in each cycle and the dynamic stiffness of the b1 were sensitive to changes in activation phase. These results raise questions concerning the factors underlying negative work output by the b1 and its function during flight. First, is negative work a consequence of either high strain rates or high frequency alone? Or, does net energy absorption per cycle reflect intrinsic specializations of the b1 muscle? Second, how are the phase-sensitive mechanical properties of the b1 related to its function in flight control?

Negative work output

We are confident that negative work output by the b1 at wing-beat frequency represents a relevant physiological performance characteristic and is not an experimental artifact. Even at low strains, the b1 work output was negative at 100 and 150 Hz for experimental series immediately preceded and followed by series at 10 or 50 Hz, during which the muscle generated net positive work. At a strain amplitude of 2 %, maximum values of work and power output by the b1 muscle at 10 Hz, $2.4 \, \mathrm{J \, kg^{-1} \, cycle^{-1}}$ ($24 \, \mathrm{W \, kg^{-1}}$), and at 50 Hz, $1.0 \, \mathrm{J \, kg^{-1} \, cycle^{-1}}$ ($50 \, \mathrm{W \, kg^{-1}}$), are within the range of values measured from other synchronous insect muscles: $1.52 \, \mathrm{J \, kg^{-1} \, cycle^{-1}}$ ($37 \, \mathrm{W \, kg^{-1}}$) for the metathoracic flight muscles of tettigoniid insects at 25 Hz and 30 °C (Josephson, 1985), $2 \, \mathrm{J \, kg^{-1} \, cycle^{-1}}$ ($45 \, \mathrm{W \, kg^{-1}}$) for the direct dorsoventral flight muscles of hawk moths at 20 Hz and 30 °C (Stevenson and Josephson, 1990) and $2.1 \, \mathrm{J \, kg^{-1} \, cycle^{-1}}$ ($52 \, \mathrm{W \, kg^{-1}}$) for locust flight muscle at 25 Hz and 30 °C (Mizisin and Josephson, 1987). All the muscles studied previously generate net positive work and power in the frequency range of their normal function. For the b1 of *Calliphora*, however, the frequency range for positive work and power was far below the frequency at which the muscle functions during flight.

In general, negative work output would be expected from any muscle subjected to excessively high strain rates. Because of the inverse relationship between shortening velocity and a muscle's capacity to generate force, the ability of a muscle to perform positive work should decrease at higher frequencies. We currently do not have direct measurements of the amplitude of b1 oscillations during flight. Consequently, we tested the b1 over a large range of strain magnitudes. Work output of the b1 was negative even at strains as small as 0.3 %, indicating that it is unlikely that the b1 performs positive work during flight by operating at very small strains.

The twitch duration of the b1 relative to the length of the cycle period may be the most important factor determining its work output. In order to perform the greatest positive work, a muscle should be maximally activated during shortening, and activation should be restricted to the shortening half-cycle. The isometric twitch duration of the b1 muscle of *Calliphora* at 23 °C exceeds the cycle period at frequencies above 17 Hz, indicating that the intrinsic characteristics which determine the twitch kinetics of the b1 may

preclude the generation of net positive work and power at wing-beat frequency. However, the frequency at which the work output of the b1 becomes negative lies below the limiting frequency for positive work output by other synchronous muscles. For example, cicada tymbal muscles have extremely brief twitch durations, and these muscles generate positive power for song production at frequencies as high as 500 Hz (Josephson and Young, 1985). The mesothoracic, first tergocoxal muscle (Tcx1) of tettigoniid insects has a significantly shorter twitch duration than the b1 of *Calliphora* at 25 °C (8.6 ms compared with 51.3 ms, onset to 90 % relaxation; Josephson, 1984). At 100 Hz, (the frequency used for singing), the Tcx1 can generate positive work ($0.18 \, \text{J kg}^{-1} \text{cycle}^{-1}$; Josephson, 1985) whereas at 100 Hz, work output by the b1 was always negative. The peak twitch tension of the b1 ($40 \, \text{N cm}^{-2}$) compared with that of the Tcx1 of tettigoniids ($1.36 \, \text{N cm}^{-2}$) suggests a trade-off in the b1 for force development at the expense of twitch brevity. The twitch duration of the b1 and the proportion of muscle volume occupied by sarcoplasmic reticulum and transverse tubules (approximately 30 %, M. H. Dickinson and M. Hummon, unpublished results) are comparable to the values for muscles that operate at lower frequencies (Josephson, 1975). Clearly, negative work at flight frequency represents a design characteristic of the b1 rather than a fundamental limit on positive work generation imposed by high frequency alone.

b1 muscle function during flight

Parallel modulation of the phase of b1 activation and the phase of the ventral flip implicates the b1 in the temporal control of wing supination during turning maneuvers (Heide, 1983; Götz, 1983; Egelhaaf, 1989; Dickinson *et al.* 1983). The present results suggest a means by which the b1, though tonically active at wing-beat frequency, could nevertheless regulate certain aspects of flight control. Spikes in the left and right b1 muscles of tethered *Calliphora* can differ by 30–70 ° during visually induced turning maneuvers (Heide, 1983). In our experiments, phase shifts of 30–70 ° correspond to changes in the work output per cycle of approximately 10–30 % within the steepest region of the work *versus* phase relationship. The same range of phase values correspond to an 8–20 % change in the peak muscle force in each cycle. Phase-dependent changes in muscle stiffness during steering maneuvers might regulate the magnitude and the timing of the oscillations of the basalare, thereby changing the mechanics of the wing hinge and causing alterations in wing kinematics. The dipteran wing hinge has been studied extensively (e.g. Miyan and Ewing, 1988; Ennos, 1987; Pfau, 1987; Wisser, 1987; Nalbach, 1989) but, because of the complex dynamics of the wing hinge during flight, we are at present unable to determine the mechanism by which variations in basalare oscillations could modulate wing kinematics. We are currently attempting to make simultaneous measurements of wing and basalare kinematics during flight that may enable us to interpret the function of the b1 muscle more precisely (M. S. Tu and M. H. Dickinson, in preparation).

Negative work output by the b1 may reflect a compromise in muscle design between the demands of multiple functions during flight. In addition to its probable role in phasically modulating wing kinematics, the b1 may have an additional tonic function during flight. Several authors have described the b1 as a wing extensor, pulling the wing

from rest into flight position (see Wisser and Nachtigall, 1984). This function, deduced on the basis of morphological investigations, may correspond to a tonic role in configuring the wing hinge during flight. Nalbach (1989) has identified the b1 as one of the muscles involved in switching the wing hinge between operating modes that produce different wing-stroke amplitudes. We have made similar observations during flight attempts by tethered flies after removing the cuticle overlying the b1. During bouts of flight, the b1 occasionally becomes quiescent even though the power muscles continue to fire. Under these conditions, the wings vibrate in their rest position and do not engage in the ventral portion of the wing stroke. Bursts of b1 activity, indicated by tonic shortening of the muscle, coincide with an abrupt switch in wing kinematics to the normal wing beat. These preliminary observations suggest that tonic force generation by the b1 may be necessary to set the wing hinge in a configuration that permits the asynchronous power muscles to drive the wings through the complete stroke cycle. The contraction kinetics of the b1 may reflect this requirement for tonic force generation during flight. The required level of tension may necessitate a twitch duration long enough to produce sufficient summation of twitch forces. The relatively long twitch duration in turn may constrain the b1 to the production of negative work at flight frequency.

Stretch activation allows the indirect flight muscles to generate the power required for flight at high wing-beat frequencies. However, the muscles responsible for flight control must be directly responsive to neural input and are, therefore, subject to the conventional trade-offs in muscle design between twitch brevity, force generation and endurance (Josephson and Young, 1987; Josephson, 1975). Rapid control of flight maneuvers in flies, however, may require repetitive activation of the steering muscles at rates equal to the contraction frequency of the power muscles. The functions of the b1 during flight, however, may require the ability to generate a substantial level of tonic tension as well as sensitivity to phasic modulation. In addition, the ability of *Drosophila* to execute continuous course corrections during flight bouts as long as 36 h implies that the b1 also has extraordinary endurance (Götz, 1987). The specializations at the subcellular level that may be necessary to allow this muscle to exert both phasic and tonic influences on the wing hinge could be fundamentally incompatible with positive power output. Negative work output by the b1 muscle may reflect general constraints in muscle design applied to a muscle that performs multiple functions under extreme conditions.

References

Bergmann-Erb, D. and Heide, G. (1990). Kontraktionsmodus direkter Flugsteuermuskeln von *Calliphora. Proceedings of the 18th Göttingen Neurobiology Conference* (ed. N. Elsner and G. Roth), p. 41. Stuttgart: Thieme Verlag.

Dickinson, M. H. (1994). The effects of wing rotation on unsteady aerodynamic performance at low Reynolds numbers. *J. exp. Biol.* (in press).

Dickinson, M. H., Lehmann, F.-O. and Götz, K. G. (1993). The active control of wing rotation by *Drosophila. J. exp. Biol.* **182**, 173–189.

EGELHAAF, M. (1989). Visual afferences to flight steering muscles controlling optomotor responses of the fly. *J. comp. Physiol.* A **165**, 719–730.

ENNOS, R. E. (1987). A comparative study of the flight mechanism of Diptera. *J. exp. Biol.* **172**, 355–372.

ENNOS, R. E. (1989). The kinematics and aerodynamics of the free flight of some Diptera. *J. exp. Biol.* **142**, 49–85.

EWING, A. W. (1979a). The neuromuscular basis of courtship song in *Drosophila*: The role of the direct and axillary wing muscles. *J. comp. Physiol.* **130**, 87–93.

EWING, A. W. (1979b). The role of feedback during singing and flight in *Drosophila*. *Physiol. Ent.* **4**, 329–337.

GÖTZ, K. G. (1983). Bewegungssehen und Flugsteuerung bei der Flege *Drosophila*. In *Insect Flight* (ed. W. Nachtigall). Stuttgart: Fischer (*Biona-report 2*, pp. 21–34).

GÖTZ, K. G. (1987). Course-control, metabolism and wing interference during ultralong tethered flight in *Drosophila melanogaster*. *J. exp. Biol.* **128**, 35–46.

HEIDE, G. (1968). Flugsteuerung durch nicht-fibrilläre Flugmuskeln bei der Schmeißfliege *Calliphora*. *Z. vergl. Physiol.* **59**, 456–460.

HEIDE, G. (1971). Die Funktion der nicht-fibrillären Flugmuskeln von *Calliphora*. Teil II. Muskuläre Mechanismen der Flugssteuerung und ihre nervöse Kontrolle. *Zool. Jb. Physiol.* **76**, 99–137.

HEIDE, G. (1975). Properties of a motor output system involved in the optomotor response in flies. *Biol. Cybernetics* **20**, 99–112.

HEIDE, G. (1983). Neural mechanisms of flight control in Diptera. In *Insect Flight* (ed. W. Nachtigall). Stuttgart: Fischer (*Biona-report 2*, pp. 35–52).

JOSEPHSON, R. K. (1975). Extensive and intensive factors determining the performance of striated muscle. *J. exp. Zool.* **194**, 135–154.

JOSEPHSON, R. K. (1984). Contraction dynamics of flight and stridulatory muscles of tettigoniid insects. *J. exp. Biol.* **108**, 77–96.

JOSEPHSON, R. K. (1985). Mechanical power output from striated muscle during cyclic contraction. *J. exp. Biol.* **114**, 493–512.

JOSEPHSON, R. K. (1993). Contraction dynamics and power output of skeletal muscle. *A. Rev. Physiol.* **55**, 527–546.

JOSEPHSON, R. K. AND YOUNG, D. (1985). A synchronous insect muscle with an operating frequency greater than 500 Hz. *J. exp. Biol.* **118**, 185–208.

JOSEPHSON, R. K. AND YOUNG, D. (1987). Fiber ultrastructure and contraction kinetics in insect fast muscles. *Am. Zool.* **27**, 991–1000.

KING, D. G. AND TANOUYE, M. A. (1983). Anatomy of motor axons to direct flight muscles in *Drosophila*. *J. exp. Biol.* **105**, 231–239.

KUTSCH, W. AND HUG, W. (1981). Dipteran flight motor pattern: Invariabilities and changes during postlarval development. *J. Neurobiol.* **12**, 1–14.

MACHIN, K. E. AND PRINGLE, J. W. S. (1960). The physiology of insect fibrillar muscle. II. The effect of sinusoidal changes of length on a beetle flight muscle. *Proc. R. Soc. B* **152**, 311–330.

MEYHÖFFER, E. AND DANIEL, T. (1990). Dynamic mechanical properties of extensor muscle cells of the shrimp *Pandalus danae*: cell design for escape locomotion. *J. exp. Biol.* **151**, 435–452.

MIYAN, J. A. AND EWING, A. W. (1984). A wing synchronous receptor for the dipteran flight motor. *J. Insect Physiol.* **30**, 567–574.

MIYAN, J. A. AND EWING, A. W. (1988). Further observations on dipteran flight: details of the mechanism. *J. exp. Biol.* **136**, 229–241.

MIZISIN, A. P. AND JOSEPHSON, R. K. (1987). Mechanical power output of locust flight muscle. *J. comp. Physiol.* A **160**, 413–419.

NALBACH, G. (1989). The gear change mechanism of the blowfly (*Calliphora erythrocephala*) in tethered flight. *J. comp. Physiol.* A **165**, 321–331.

PFAU, H. K. (1987). Critical comments on a 'Novel mechanical model of dipteran flight' (Miyan and Ewing, 1985). *J. exp. Biol.* **128**, 463–468.

PRINGLE, J. W. S. (1949). The excitation and contraction of the flight muscles of insects. *J. Physiol., Lond.* **108**, 226–232.

STEVENSON, R. D. AND JOSEPHSON, R. K. (1990). Effects of operating frequency and temperature on mechanical power output from moth flight muscle. *J. exp. Biol.* **149**, 61–78.

WISSER, A. (1987). Mechanisms of wing rotating regulation in *Calliphora erythrocephala* (Insecta, Diptera). *Zoomorph.* **109**, 261–268.

WISSER, A. AND NACHTIGALL, W. (1984). Functional-morphological investigations on the flight muscles and their insertion points in the blowfly *Calliphora erythrocephala* (Insecta, Diptera). *Zoomorph.* **104**, 188–195.